

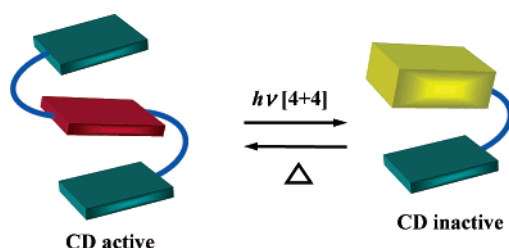
Naphthalene- and Anthracene-Based Aromatic Foldamers with Iminodicarbonyl Linkers: Their Stabilities and Application to a Chiral Photochromic System Using Retro [4 + 4] Cycloaddition

Hyuma Masu,[†] Ikuko Mizutani,[‡] Takako Kato,[†] Isao Azumaya,[†] Kentaro Yamaguchi,[†]
Keiki Kishikawa,[‡] and Shigeo Kohmoto^{*,‡}

Department of Applied Chemistry and Biotechnology, Faculty of Engineering, Chiba University, 1-33, Yayoi-cho, Inage-ku, Chiba 263-8522, Japan and Faculty of Pharmaceutical Sciences at Kagawa Campus, Tokushima Bunri University, 1314-1, Shido, Sanuki, Kagawa 769-2193, Japan

kohmoto@faculty.chiba-u.jp

Received June 2, 2006



A circular dichroism (CD) spectral study on chiral aromatic chain imides possessing anthracene and naphthalene moieties with bulky N substituents showed that their helical chirality based on folding remained for a reasonably long time without racemization in solution. Racemization due to conformational equilibration occurred very slowly, requiring over 1 week at ambient temperature. Their CD spectra both in solution and in the solid state gave similar CD signals, suggesting retention of helicity observed in the solid state even after dissolving. As an application of this novel chiral folding of aromatic chain imides, a chiral photochromic system was investigated based on the photo [4 + 4] cycloaddition and its thermal cycloreversion of an anthracene–naphthalene system. The foldamer possessing an anthracene moiety in the center connected with two naphthalene moieties below and above it by iminodicarbonyl linkers was prepared for this purpose. Induced CD was observed for the foldamer with (*S*)-1-(1-naphthyl)ethyl substituents at the imide nitrogen atoms. Chiral photochromic cycles were monitored by CD spectral measurement.

Introduction

In recent years, much work has been done to explore new types of artificial higher order structures in order to understand and mimic the secret of elaborate biological systems.¹ One of the key structural elements of a unique three-dimensional structure of biological macromolecules is folding governed by hydrogen bonds, electrostatic interactions, and hydrophobic

forces. By applying these interactions, a variety of foldamers with unique structural features have been prepared.² Our interest is to develop a helically chiral folding building block with conformational stability, which contributes in designing chiral self-assembled foldamers.³ To the best of our knowledge, there is no report on a simple chiral foldamer without an asymmetric

[†] Tokushima Bunri University.

[‡] Chiba University.

(1) (a) Hill, R. B.; Raleigh, D. P.; Lombardi, A.; Degrado, W. F. *Acc. Chem. Res.* **2000**, *33*, 745–754. (b) Nakano, T.; Okamoto, Y. *Chem. Rev.* **2001**, *101*, 4013–4038. (c) Lan, T.; McLaughlin, L. W. *Biochemistry* **2001**, *40*, 968–976. (d) Brooks, C. L., III *Acc. Chem. Res.* **2002**, *35*, 447–454. (e) Straub, J. E.; Guevara, J.; Huo, S.; Lee, J. P. *Acc. Chem. Res.* **2002**, *35*, 473–481. (f) Wang, W.; Wan, W.; Zhou, H.-H.; Niu, S. Li, A. D. Q. *J. Am. Chem. Soc.* **2003**, *125*, 5248–5249.

(2) (a) Gellman, S. H. *Acc. Chem. Res.* **1998**, *31*, 173–180. (b) Hill, D. J.; Mio, M. J.; Prince, R. B.; Hughes, T. S.; Moore, J. S. *Chem. Rev.* **2001**, *101*, 3893–4011. (c) Li, A. D. Q.; Wang, W.; Wang, L.-Q. *Chem. Eur. J.* **2003**, *9*, 4594–4601. (d) Schmuck, C. *Angew. Chem.* **2003**, *115*, 2552–2556; *Angew. Chem., Int. Ed.* **2003**, *42*, 2448–2452. (e) Ernst, J. T.; Becerril, J.; Park, H. S.; Yin, H.; Hamilton, A. D. *Angew. Chem.* **2003**, *115*, 553–557; *Angew. Chem., Int. Ed.* **2003**, *42*, 535–539. (f) Goto, H.; Heemstra, J. M.; Hill, D. J.; Moore, J. S. *Org. Lett.* **2004**, *6*, 889–892. (g) Zhao, X.; Jia, M.-X.; Jiang, X.-K.; Wu, L.-Z.; Li, Z.-T.; Chen, G.-J. *J. Org. Chem.* **2004**, *69*, 270–279. (h) Stone, M. T.; Heemstra, J. M.; Moore, J. S. *Acc. Chem. Res.* **2006**, *39*, 11–20.

center or the aid of a chiral auxiliary. It is known that the folded conformations of aromatic amide oligomers are more stable than those of aliphatic amides.⁴ Considering this, we examined the stability of the folded conformation of aromatic chain imides. Two aromatic moieties connected at the iminodicarbonyl linker may have a conformation in which they face each other due to the planarity and preferred cis conformation of an amide unit.⁵ It is also known that optically active atropisomeric aromatic amides have a long half-life for racemization in solution.⁶ Aromatic chain imides can be considered where two units of atropisomeric aromatic amides are connected. Therefore, a conformationally stable concave-shaped folding unit can be created. In our previous study, we found that aromatic chain imides **1** and **2** gave chiral crystals upon recrystallization though the molecules have no asymmetric carbon.⁷ They had concave-shaped folded conformations in crystals examined by single-crystal X-ray analysis. We have been interested in the stability of their folded conformations and whether the helical chirality observed in the crystalline state can be preserved even in solution.⁸ In the first part of this paper we report on the simplest chiral concave-shaped foldamer (or a unit of foldamer) which shows reasonably stable helical chirality even in solution at ambient temperature. In the last part of the paper, we report on the application of this concave-shaped aromatic foldamer to a chiral photochromic system which is used as a potent tool for nanotechnology,⁹ especially for optical data storage and processing.¹⁰ Generally, bistable molecular systems are used for this purpose. The cis–trans photoisomerization of sterically overcrowded alkenes is among the most extensively studied example.¹¹ The cis–trans photoisomerization of pendant azobenzenes is frequently utilized in liquid crystalline polymers for

this purpose.¹² Recently, the reaction was applied to molecular shuttles.¹³ In addition to these applications, the 1,6-electrocyclization of diarylethenes¹⁴ and fulgides,¹⁵ typical photochromic systems, have been applied as well. A few examples employ redox systems.¹⁶ In light of the progress in this area, an entry of a novel chiral photochromic system based on a new concept using hitherto unexplored reactions is highly desirable. Foldamers containing chromophoric functionalities are of current interest.¹⁷ Cyclodimers of coumarin¹⁸ and anthracene¹⁹ are well known to show their retro cycloreversion. A difficulty associated with applying an aromatic [4 + 4] cycloadduct for a chiral photochromic system is control of molecular chirality after retro cycloreversion. To keep the molecular chirality to manifest its induced CD in solution, the geometrical relation of two aromatic moieties regenerated by cycloreversion should be the same as the original one with the same helicity. This is hard to accomplish with a linearly tethered molecule due to its flexibility. In view of this, we considered that the conformational stability of aromatic chain imides is useful for creation of a new chiral photochromic system.

Herein, we report the construction of a simple helically chiral foldamer unit and its application to a novel chiral photochromic system based on aromatic [4 + 4] photocycloaddition.⁷

Results and Discussion

Conformational Stability of Concave-Shaped Chiral Aromatic Chain Imides in Solution. The CD spectra of six chiral aromatic chain imides,²⁰ (*P*)-**1**, (*P*)-**2**, (*M*)-**2**, (*P*)-(*R*)-**3**, (*M*)-

(3) (a) Piguet, C.; Bernardinelli, G.; Hopfgartner, G. *Chem. Rev.* **1997**, *97*, 2005–2062. (b) Ohkita, M.; Lehn, J.-M.; Baum, G.; Fenske, D. *Chem. Eur. J.* **1999**, *5*, 3471–3481. (c) Fuhrhop, J.-H.; Wang, T. *Chem. Rev.* **2004**, *104*, 2901–2938.

(4) (a) Marsella, M. J.; Kim, I. T.; Tham, F. J. *Am. Chem. Soc.* **2000**, *122*, 974–975. (b) Nakamura, K.; Okubo, H.; Yamaguchi, M. *Org. Lett.* **2001**, *3*, 1097–1099. (c) Adams, H.; Hunter, C. A.; Lawson, K. R.; Perkins, J.; Spev, S. E.; Urch, C. J.; Sanderson, J. M. *Chem. Eur. J.* **2001**, *7*, 4863–4878. (d) Zhao, D.; Moore, J. S. *J. Org. Chem.* **2002**, *67*, 3548–3554. (e) Huc, I. *Eur. J. Org. Chem.* **2004**, 17–29.

(5) (a) Yamaguchi, K.; Matsumura, G.; Kagechika, H.; Azumaya, I.; Ito, Y.; Itai, A.; Shudo, K. *J. Am. Chem. Soc.* **1991**, *113*, 5474–5475. (b) Itai, A.; Toriumi, Y.; Saito, S.; Kagechika, H.; Shudo, K. *J. Am. Chem. Soc.* **1992**, *114*, 10649–10650. (c) Kohmoto, S.; Masu, H.; Tatsuno, C.; Kishikawa, K.; Yamamoto, M.; Yamaguchi, K. *J. Chem. Soc., Perkin Trans. I* **2000**, 4464–4468.

(6) (a) Clayden, J.; Pink, J. H. *Tetrahedron Lett.* **1997**, *38*, 2561–2564. (b) Clayden, J.; Mitjans, D.; Yousset, L. H. *J. Am. Chem. Soc.* **2002**, *124*, 5266–5267.

(7) Kohmoto, S.; Ono, Y.; Masu, H.; Yamaguchi, K.; Kishikawa, K.; Yamamoto, M. *Org. Lett.* **2001**, *3*, 4153–4155.

(8) (a) Azumaya, I.; Yamaguchi, K.; Okamoto, I.; Kagechika, H.; Shudo, K. *J. Am. Chem. Soc.* **1995**, *117*, 9083–9084. (b) Tabei, J.; Nomura, R.; Masuda, T. *Macromolecules* **2003**, *36*, 573–577.

(9) (a) Feringa, B. L.; Delden, R. A.; Koumura, N.; Geertsema, E. M. *Chem. Rev.* **2000**, *100*, 1789–1816. (b) Chen, C.-T.; Chou, Y.-C. *J. Am. Chem. Soc.* **2000**, *122*, 7662–7672. (c) Nakashima, H.; Fujiki, M.; Koe, J. R.; Motonaga, M. *J. Am. Chem. Soc.* **2001**, *123*, 1963–1969. (d) Braga, S. F.; Galvão, D. S.; Barone, P. M. V. B.; Dantas, S. O. *J. Phys. Chem. B* **2001**, *105*, 8334–8338. (e) Fenniri, H.; Deng, B. L.; Ribbe, A. E. *J. Am. Chem. Soc.* **2002**, *124*, 11064–11072.

(10) (a) Green, M. M.; Cheon, K.-S.; Yang, S.-Y.; Park, J.-W.; Swansburg, S.; Liu, W. *Acc. Chem. Res.* **2001**, *34*, 672–680. (b) Sakamoto, M.; Iwamoto, T.; Nono, N.; Ando, M.; Arai, W.; Mino, T.; Fujita, T. *J. Org. Chem.* **2003**, *68*, 942–946. (c) Goto, H.; Zhang, H. Q.; Yashima, E. *J. Am. Chem. Soc.* **2003**, *125*, 2516–2523. (d) Saxena, A.; Guo, G.; Fujiki, M.; Yang, Y.; Ohira, A.; Okoshi, K.; Naito, M. *Macromolecules* **2004**, *37*, 3081–3083. (e) Yashima, E.; Maeda, K.; Nishimura, T. *Chem. Eur. J.* **2004**, *10*, 42–51.

(11) (a) Huck, N. P. M.; Jager, W. F.; Feringa, B. L. *Science* **1996**, *273*, 1686–1688. (b) Zijlstra, R. W. J.; Jager, W. F.; Lange, B.; Duijnen, P. T.; Feringa, B. L.; Goto, H.; Saito, A.; Koumura, N.; Harada, N. *J. Org. Chem.* **1999**, *64*, 1667–1674.

(12) (a) Moriyama, M.; Tamaoki, N. *Chem. Lett.* **2001**, 1142–1143. (b) Ichimura, K. *Chem. Rev.* **2000**, *100*, 1847–1873. (c) Bobrovsky, A. Y.; Boiko, N. I.; Shibaev V. P. *Chem. Mater.* **2001**, *13*, 1998–2001. (d) Kim, M.-J.; Shin, B.-G.; Kim, J.-J.; Kim, D.-Y. *J. Am. Chem. Soc.* **2002**, *124*, 3504–3505.

(13) (a) Bottari, G.; Leigh, D. A.; Pérez, E. M. *J. Am. Chem. Soc.* **2003**, *125*, 13360–13361. (b) Altieri, A.; Gatti, F. G.; Kay, E. R.; Leigh, D. A.; Martel, D.; Paolucci, F.; Slawin, A. M. Z.; Wong, J. K. Y. *J. Am. Chem. Soc.* **2003**, *125*, 8644–8654. (c) Qu, D.-H.; Wang, Q.-C.; Ren, J.; Tian, H. *Org. Lett.* **2004**, *6*, 2085–2088.

(14) (a) Kobatake, S.; Yamada, M.; Yamada, T.; Irie M. *J. Am. Chem. Soc.* **1999**, *121*, 8450–8456. (b) Kodani, T.; Matsuda, K.; Yamada, T. Kobatake, S.; Irie M. *J. Am. Chem. Soc.* **2000**, *122*, 9631–9637. (c) Irie, M. *Chem. Rev.* **2000**, *100*, 1685–1716. (d) Mitchell, R. H.; Brkic, Z.; Sauro, V. A.; Berg, D. J. *J. Am. Chem. Soc.* **2003**, *125*, 7581–7585. (e) Matsuda, K.; Takayama, K.; Irie, M. *Inorg. Chem.* **2004**, *43*, 482–489.

(15) (a) Heller, G. H.; Oliver, S. *J. Chem. Soc., Perkin Trans. I* **1981**, 197–201. (b) Darcy, P. J.; Heller, G. H.; Strydom, P. J.; Whittall, J. *J. Chem. Soc., Perkin Trans. I* **1981**, 202–205. (c) Yokoyama, Y. *Chem. Rev.* **2000**, *100*, 1717–1739. (d) Liang, Y.; Dvornikov, A. S.; Rentzepis, P. M. *Macromolecules* **2002**, *35*, 9377–9382.

(16) Nakajima, R.; Tsuruta, M.; Higuchi, M.; Yamamoto, K. *J. Am. Chem. Soc.* **2004**, *126*, 1630–1631.

(17) Han, J. J.; Wang, W.; Li, A. D. Q. *J. Am. Chem. Soc.* **2006**, *128*, 672–673.

(18) (a) McCullough, J. J. *Chem. Rev.* **1987**, *87*, 811–860. (b) Mal, N. K.; Fujiwara, M.; Tanaka, Y.; Taguchi, T.; Matsukawa, M. *Chem. Mater.* **2003**, *15*, 3385–3394. (c) Motoyanagi, J.; Fukushima, T.; Ishii, N.; Aida, T. *J. Am. Chem. Soc.* **2006**, *128*, 4220–4221.

(19) (a) Bouas-Laurent, H.; Castellán, A.; Desvergne, J.-P. *Pure Appl. Chem.* **1980**, *52*, 2633–2648. (b) Becker, H.-D. *Chem. Rev.* **1993**, *93*, 145–172. (c) Bouas-Laurent, H.; Castellán, A.; Desvergne, J.-P.; Lapouyade, R. *Chem. Soc., Rev.* **2000**, *29*, 43–55. (d) Bouas-Laurent, H.; Castellán, A.; Desvergne, J.-P.; Lapouyade, R. *Chem. Soc. Rev.* **2001**, *30*, 248–263. (e) Cicogna, F.; Ingrassio, G.; Lodato, F.; Marchetti, F.; Zandomenghi, M. *Tetrahedron* **2004**, *60*, 11959–11968.

(20) The known chiral aromatic chain imides were prepared according to the previously reported method (refs 5c and 7).

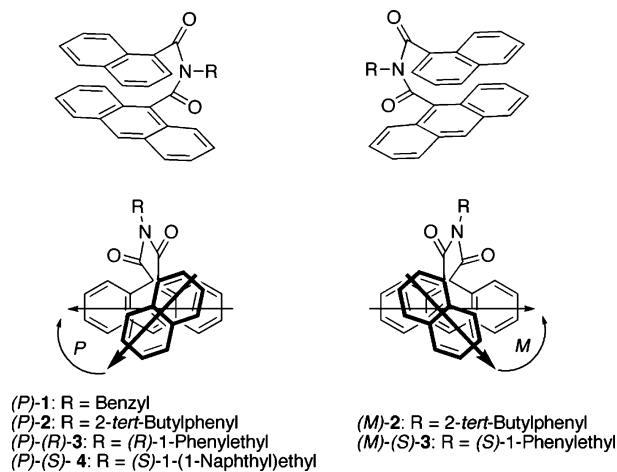


FIGURE 1. Chiral aromatic chain imides possessing anthracene and naphthalene moieties.

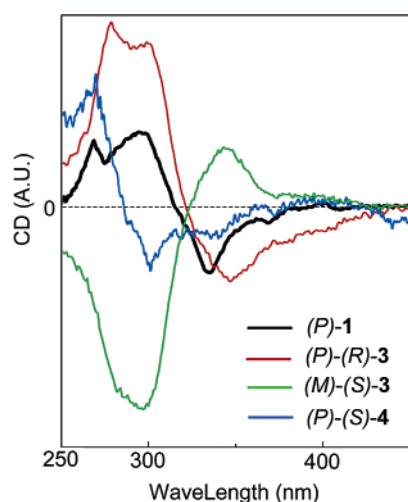


FIGURE 2. Solid-state CD spectra of (*P*)-1, (*P*)-(*R*)-3, (*M*)-(*S*)-3, and (*P*)-(*S*)-4 (KBr). Due to noticeable noise, the spectra could not be measured precisely in the region below 250 nm.

(*S*)-3, and (*P*)-(*S*)-4 (Figure 1), were examined in the solid state and CHCl_3 (Figures 2 and 3). Although imides **1** and **2** have no chiral center, they gave enantiomeric chiral crystals upon recrystallization. Imides (*P*)-(*R*)-3, (*M*)-(*S*)-3, and (*P*)-(*S*)-4 possess chiral substituents at the imide nitrogen atoms. Their helicities were determined based on the single-crystal X-ray structure of **3** reported previously^{5c} with the (*S*)-1-phenylethyl substituent at the imide nitrogen atom. Its helicity was determined to be (*M*).

Consequently, the helicity of the other diastereomer of **3** with the (*R*)-1-phenylethyl substituent was assigned to be (*P*). The helicity of other carboxamides were assigned based on their CD signals in comparison with those of (*P*)-(*R*)-3 and (*M*)-(*S*)-3.

The solid-state CD spectra were recorded on their KBr pellets. The pellets were prepared by grinding ca. 1 mg of imide and ca. 10 mg of dry KBr powder followed by pressing under vacuum. Unlike in solution, all compounds showed CD signals in the solid state. Figure 2 shows the solid-state (KBr) CD spectra of (*P*)-1, (*P*)-(*R*)-3, (*M*)-(*S*)-3, and (*P*)-(*S*)-4. A similar CD spectral pattern is observed for (*P*)-1 and (*P*)-(*R*)-3, which indicates that they have the same helicity. Almost mirror images of CD spectra were observed between (*P*)-(*R*)-3 and (*M*)-(*S*)-3.

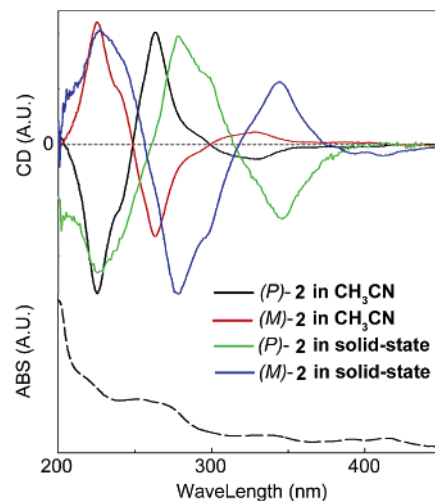


FIGURE 3. CD spectra of (*P*)-2 and (*M*)-2 in solution (CH_3CN) and in the solid state (KBr). Absorption spectrum of **2** in the solid state (KBr) is indicated by dashed lines.

A different CD spectral pattern is observed for (*P*)-(*S*)-4. The region from 250 to 315 nm is composed of both induced CD as well as intrinsic CD signal by the chiral naphthyl substituent, while the region between 315 and 400 nm is solely due to exciton coupling of the anthryl and naphthyl chromophores. The sign of Cotton effect of its long-wavelength band is the same as those of (*P*)-1 and (*P*)-(*R*)-3. The helicity of (*P*)-(*S*)-4 is determined based on this long-wavelength band. Induced CD signals originate in the exciton coupling between the anthryl and naphthyl chromophores.²¹ The chiral auxiliaries regulate their chiral orientation, but they are not the chromophore responsible for the induced CD signals. The bulkiness of the N substituent seems to affect significantly the orientation of these two chromophores in the solid state. While (*P*)-(*S*)-4 possesses *P* helicity, the CD signal corresponding to *M* helicity has been observed for (*M*)-(*S*)-3. Thus, the observed CD signals are not consistent to the absolute configuration of the chiral auxiliaries at the imide nitrogen atoms.

Only (*P*)-2, (*M*)-2, and (*P*)-(*S*)-4 showed CD spectra in solution, whereas no CD signal was observed for (*P*)-1, (*P*)-(*R*)-3, and (*M*)-(*S*)-3 in solution. Bulkiness of the N substituents could play a crucial role in displaying CD in solution. Because of a lack of steric hindrance by the N substituents, (*P*)-1, (*P*)-(*R*)-3, and (*M*)-(*S*)-3 could have a flexible conformation in solution. Therefore, immediate racemization or epimerization occurs to result in the observation of no CD signal. As shown in Figure 3, enantiomeric chiral crystals of (*P*)-2 and (*M*)-2 gave CD signals of mirror images as well as in the solid state. Slightly red-shifted CD spectra were observed in the solid state compared to those in solution. The retention of helicity in the solid state even after dissolving in solution was confirmed by employing a relatively large single crystal of (*P*)-2. One single crystal of (*P*)-2 (ca. 8 mg) was cut into two pieces. The CD spectral measurement was carried out in the solid state for one piece and in solution for the other piece. Identical signs of Cotton effect and the similar shape of CD spectra were observed for both pieces. The results indicate that their folded conformations in crystals are retained after dissolving in solution.

(21) Snatzke, G. *Angew. Chem., Int. Ed. Engl.* **1979**, *18*, 363–377.

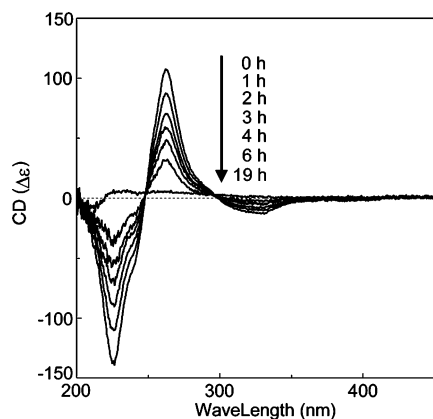
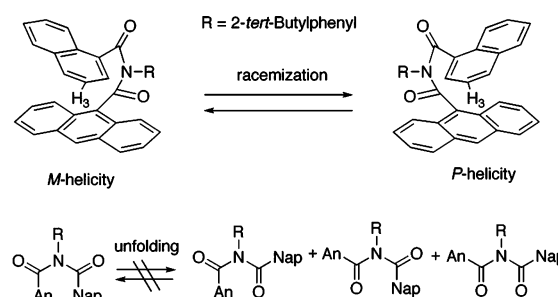


FIGURE 4. CD spectral changes of (*P*)-**2** standing at 70 °C in CH₃CN.

Though **2** and **4** possess a fairly stable helical conformation in solution, they gradually lose their CD signals after standing at room temperature for a long time. Figure 4 shows the CD spectral change of (*P*)-**2** at 70 °C in CH₃CN. Its induced CD corresponding to the exciton coupling based on the absorption (ca. 250 nm) along the long axes of the anthracene and naphthalene moieties indicated that the molecule has *P* helicity. It can be confirmed also from the fact that (*P*)-**2** has a similar pattern for the CD spectrum to those of (*P*)-**1**, (*P*)-(*R*)-**3**, and (*P*)-(*S*)-**4**. The results indicated that (*P*)-**2** was gradually losing its CD signal. The kinetic study of the disappearance of CD signal of (*P*)-**2** was carried out by measuring the decrease of $\Delta\epsilon$ at 263 nm in CH₃CN. A fairly large E_a (27.9 kcal/mol) of the disappearance of CD was observed. Recently, the frozen chirality of a similar type of compounds was reported on chiral crystals of an achiral asymmetrically substituted imide with a tetrahydronaphthyl group on the nitrogen atom.²² In that case, the CD signal observed in its crystalline state quickly disappeared in THF with a half-life of 7.8 min at -20 °C. Even though its half-life is very short, it is exceptionally stable for this type of compound. There was an indication of such a frozen chirality of aromatic amides in cold solution.^{8a} Chiral hosts could assist fixation of chiral conformation of amides at low temperature.²³ Our example is extremely stable compared with those of similar types of compounds. Because of the bulky substituent at the nitrogen atom, the CD signal of (*P*)-(*S*)-**4** remained without change even after refluxing in CH₃CN for 2 weeks in a sealed tube. The results show a marked contrast to (*P*)-(*R*)-**3** and (*M*)-(*S*)-**3**, which showed no CD in solution. The results clearly show that the bulkiness of the N substituent governs the stability of helical conformation.

Two possible explanations could be considered for the disappearance of the CD signals of **2** after standing for a long time: (1) racemization while keeping their folding conformations intact and (2) conformational changes due to rotation around the single bonds, which results in unfolding of its conformation (Scheme 1). To investigate the cause of this, we carried out their ¹H NMR spectral study before and after heating. If no spectral change is observed, racemization is the origin. If unfolding of their conformations takes place, shielding caused by the overlapping of naphthalene and anthracene moieties will

SCHEME 1. Racemization of **2** in Solution



disappear. A distinct downfield shift should be observed²⁴ for the most shielded proton (H₃ at δ 6.30 in CDCl₃). Its ¹H NMR spectra recorded after the disappearance of CD were identical to those before heating. Moreover, the characteristic fluorescence of the naphthalene–anthracene exciplex (λ_{em} 482 nm in CH₃CN) due to the folding conformation remained without change. Therefore, we conclude that disappearance of the CD signal of **2** is caused by racemization and its conformation is kept folded.

Unlike atropisomers, in general, it is hard to keep the optical activity of imides based on the molecular chirality without racemization after dissolving it in solution since they possess multiple flexible single bonds. To keep the helically folded conformation in solution, introduction of noncovalent interactions is generally required, such as intramolecular hydrogen bonding commonly employed in β -peptides.²⁵ In our case, electrostatic repulsion between carbonyls settles the folded conformation with the assistance of π – π interaction and steric hindrance due to the bulky groups substituted at the imide nitrogen atom, which may be the driving force to prevent racemization.

Chiral Photochromic System based on Reversible [4 + 4] Photocycloaddition. During the course of our study on aromatic imide foldamers with multiple units of naphthalene moieties we found that induced CDs were generated by the helical arrangement of folding naphthalene moieties.²⁶ Unlike the concave-shaped molecules **1–3** with two units of aromatic moieties, these foldamers with more than three aromatic moieties connected with iminodicarbonyl linkers could keep their folding conformations in solution without change observed in their CD spectra. From these findings we considered that aromatic foldamers can be applied to a chiral photochromic system. As the photochromic foldamer capable of [4 + 4] cycloaddition and its cycloreversion, we prepared compounds **5a**, **5b**, and **5c** which possessed an anthracene moiety in the center and two naphthalene moieties below and above the anthracene moiety (Scheme 2).

The S-shaped folding structure was confirmed by single-crystal X-ray analysis of **5a** and **5b** (Figure 5). **5a** and **5b** gave achiral single crystals, although **1** and **2** afforded chiral crystals. For **5c**, suitable single crystals for X-ray analysis could not be obtained. The naphthalene and anthracene moieties are twisted

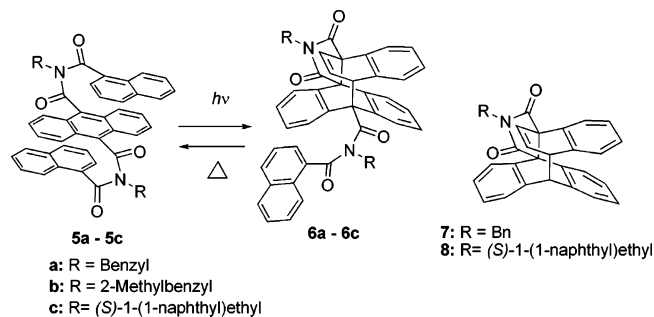
(24) Krebs, F. C.; Jørgensen, M. *J. Org. Chem.* **2002**, *67*, 7511–7518.

(22) Sakamoto, M.; Iwamoto, T.; Nono, N.; Ando, M.; Arai, W.; Mino, T.; Fujita, T. *J. Org. Chem.* **2003**, *68*, 942–946.

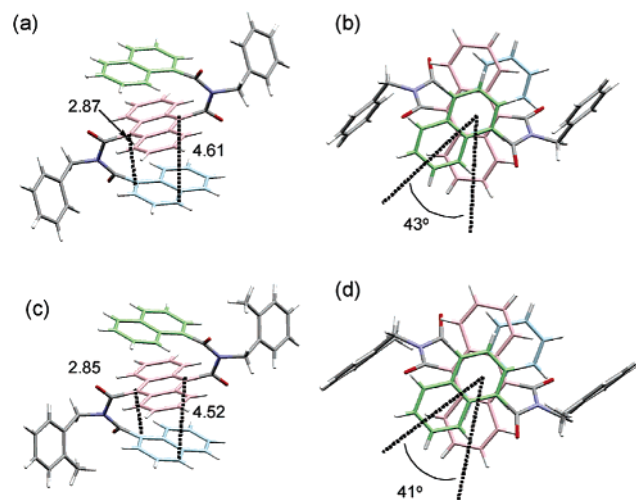
(23) Bach, T.; Grosch, B.; Strassner, T.; Herdtweck, E. *J. Org. Chem.* **2003**, *68*, 1107–1116.

(25) (a) Inai, Y.; Ishida, Y.; Tagawa, K.; Takasu, A.; Hirabayashi, T. *J. Am. Chem. Soc.* **2002**, *124*, 2466–2473. (b) Bernardi, F.; Garavelli, M.; Scatizzi, M.; Tomasini, C.; Trigari, V.; Crisma, M.; Formaggio, F.; Peggion, C.; Toniolo, C. *Chem. Eur. J.* **2002**, *8*, 2516–2525. (c) Cheng, R. P.; Gellman, S. H.; DeGrado, W. F. *Chem. Rev.* **2001**, *101*, 3219–3232. (d) Seebach, D.; Beck, A. K.; Bierbaum, D. *Chem. Biodiversity* **2004**, *1*, 1111–1239.

(26) Masu, H.; Sakai, M.; Kishikawa, K.; Yamamoto, M.; Yamaguchi, K.; Kohmoto, S. *J. Org. Chem.* **2005**, *70*, 1423–1431.

SCHEME 2. Reversible [4 + 4] Cycloaddition of S-Shaped Foldamers 5a–5c

TABLE 1. Chemical Shift Assignment of Protons of 5a

proton	chemical shift ^a
a	5.48 (s, 4H)
b	6.15 (t, <i>J</i> = 7.6, 2H)
c	6.32 (d, <i>J</i> = 6.4, 2H)
d	6.41 (d, <i>J</i> = 8.2, 2H)
e	6.63 (t, <i>J</i> = 7.6, 2H)
f	6.85 (d, <i>J</i> = 8.2, 2H)
g	7.09 (t, <i>J</i> = 7.6, 2H)
h	7.11 (m, 8H)
i	7.15 (m, 2H)
j	7.41 (t, <i>J</i> = 7.3, 2H)
k	7.48 (t, <i>J</i> = 7.3, 4H)
l	7.77 (d, <i>J</i> = 7.3, 4H)


FIGURE 5. Single-crystal X-ray structure of **5a** (side (a) and top (b) views) and **5b** (side (c) and top (d) views). Distances are indicated in Angstroms.

against each other with an angle of 43° and 41° for **5a** and **5b**, respectively, creating the folding structures. The folding occurs in a zigzag way. Satisfactory overlapping of the anthracene and naphthalene moieties was observed. The distances between the adjacent carbons of them are 2.87 and 4.61 Å for **5a** and 2.85

and 4.52 Å for **5b** as shown in Figure 5. This indicates that a facile intramolecular [4 + 4] photocycloaddition can be attained. Because of this overlapping, some of the protons of the naphthalene moiety are expected to be shielded by the anthracene moiety resulting in the upfield shifts if the molecule has the similar folded conformation in solution as in the solid state. Indeed, several protons were highly upfield shifted in their ¹H NMR spectra.

To confirm the folded conformation in solution, ¹H NMR spectral study of **5a** was carried out. Table 1 shows the assignment of the protons of **5a** based on its HH-COSY spectrum. Protons b, c, and d are highly upfield shifted. According to its single-crystal X-ray structure, these protons are located in the shielding zone of the anthracene moiety. Thereby, it is expected that the conformation of **5a** in solution is similar to that in the solid state. In addition, NOE difference spectral study also supported the folded conformation in solution. Irradiation of protons h caused NOEs on protons c and d, and vice versa. It is difficult to assign the anthracene protons responsible for these NOEs since all anthracene protons appeared together as protons h. However, it is quite natural to consider that these NOEs are caused by the nearest anthracene protons. The distance between proton c and the nearest anthracene proton is 2.91 Å, and that of proton d and the nearest anthracene proton is 3.41 Å from its single-crystal X-ray data. These distances are reasonable to consider the occurrence of NOE enhancement. Due to the complex ¹H NMR spectra it is difficult to assign the proton chemical shifts of **5b** and **5c**. However, a similar tendency of upfield shift was also observed for **5b** and **5c**.

Irradiation of **5a**, **5b**, and **5c** with a high-pressure mercury lamp in CHCl₃ through a Pyrex filter caused an immediate color change of their solution from yellow to colorless. Standing the irradiated solution of them at ambient temperature caused gradual recovery of their yellow color with a half-life of ca. 8.5 h at ca. 25 °C, 32 h at ca. 15 °C, and 50 min at ca. 25 °C for **5a**, **5b**, and **5c**, respectively. The ¹H NMR spectrum of the sample recorded immediately after irradiation at ca. 0 °C showed the peaks characteristic to the [4 + 4] cycloadducts. Their structures were identified by comparison of their ¹H NMR spectral patterns with those of the similar [4 + 4] adducts **7** and **8**,^{5c} reported previously. Figure 6 shows a comparison of the characteristic ¹H NMR chemical shifts of cycloadducts **6a** and **6c**. Similar patterns were observed for two vinylic protons H₂ and H₃ and the bridgehead proton H₄. In cycloadduct **6a**, the benzylic protons changed their chemical shifts from δ 5.48 (s) in **5a** to two sets of doublets at δ 5.18 (d, *J* = 13.8) and 5.24 (d, *J* = 13.8) and δ 4.00 (d, *J* = 14.0) and 4.05 (d, *J* = 14.0). The former corresponds to the *N*-benzylic protons of the pyrrolidine 2,5-dione ring which is almost identical to those of **7**. The remaining benzylic protons shifted upfield largely due to disappearance of the deshielding effect caused by the anthracene moiety before cycloaddition. A similar tendency was observed for **6b** and **6c**. Cycloadduct **6c** was obtained as a diastereomeric mixture in a ratio 95:5 at 0 °C in CDCl₃. The diastereoselectivity was improved slightly to 97:3 when the reaction was carried out at -40 °C. The diastereoselectivity was similar to that observed in our previous study of the photocycloaddition of **8**.⁷ Since the ¹H NMR spectra after irradiation of **5c** were complicated due to formation of the [4 + 4] cycloadduct **6c** (major) together with the minor diastereomeric cycloadduct and **5c** generated by retro cycloreversion due to

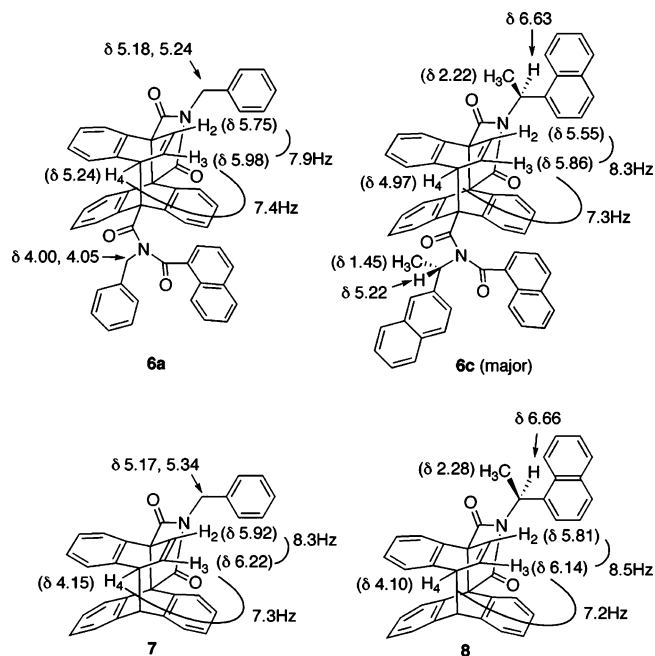


FIGURE 6. Comparison of the ¹H NMR chemical shifts (CDCl₃) of cycloadducts **6a** and **6c** with those of the known cycloadducts **7** and **8**.

instability of the cycloadduct, assignment of the peaks was carried out based on the HH–COSY spectrum of the irradiated mixture. Due to the instability of **6c**, isolation was difficult. When the CDCl₃ solution of **5a** (1.1×10^{-2} M) in a NMR tube was irradiated externally by a high-pressure mercury lamp at -40 °C, its yellow color disappeared completely. However, after measurement of the ¹H NMR spectrum, the color of the solution turned slightly yellow. The degree of the retro cyclo-reversion during the measurement was 7% based on integration. Therefore, generation of **5c** is due to its thermal instability and not because of the photochemical retro process. The photochemical reaction was a complete conversion of **5c** to **6c**, and no photostationary state was involved. Figure 7a shows the UV–vis absorption spectral changes of **5c** during irradiation. Complete conversion of **5c** was attested by the complete disappearance of the absorption band around 420 nm which was responsible for the yellow color. This disappearance is due to destruction of the overlapped p system. Since no crossing point exists in the absorption spectra of **5c** and **6c**, no isosbestic point is observed for conversion of **5c** to **6c** even though conversion proceeds in a first-order process. Thermally, the cycloadduct **6c** was completely converted to **5c**. Its CD and absorption spectra were changed to the identical spectra to those of **5c** after standing for 5.5 h at ambient temperature (ca. 25 °C) or heating for 20 min at 60 °C. The T-type photochromism (one of the reversible processes is thermal and the other is photochemical) took place. Since **5c** possesses chiral auxiliaries, cycloaddition may afford two diastereomers.

There was a large difference in stability among cycloadducts. In contrast to **6a**, **6b**, and **6c**, cycloadducts without an extra naphthoyl moiety, **7** and **8**, were stable at room temperature. It required heating at higher temperature for their retro [4 + 4] cycloaddition. For example, **7** have a half-life of 3.9 h in DMSO-*d*₆ at 130 °C measured by ¹H NMR study. We considered that this difference might arise from the steric constraint caused by the additional naphthyl moiety. ΔH of **6c** is 17.2 kcal/mol larger

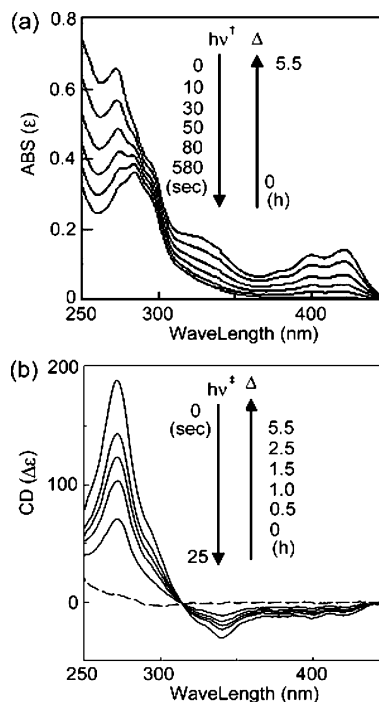


FIGURE 7. (a) Absorption spectral changes of **5c** (5.1×10^{-5} M) upon irradiation (>290 nm), changes from top to bottom, and thermal recovery of **5c** at ambient temperature (ca. 25 °C) in CHCl₃. (b) CD spectral changes of **5c** to **6c** after irradiation (>290 nm), changes from top to bottom, and thermal recovery of **5c** at ambient temperature (ca. 25 °C) in CHCl₃. †Irradiation was carried out with a high-pressure mercury lamp through a slit to slow the speed of photocycloaddition. ‡Irradiation was carried out for 25 s for completion of the cycloaddition without a slit.

than that of **5c** calculated by AM1 calculation,²⁷ indicating that **6c** is thermally less stable than **5c**.

Unlike the usual thermal retro [4 + 4] cycloreversion, that of **6c** occurred at moderate temperature, resulting in **5c** having recovery of the CD signal identical to that before the irradiation–heating cycle. The results imply that the chiral photochromic system can be created by utilizing reversible [4 + 4] cycloaddition of **5c**. No spectral change in the CD spectrum of **5c** was observed, even after heating in CHCl₃ at 60 °C for 1 day. When the CD spectrum of **5c** was measured at -45 °C, its signal intensity was slightly (ca. 20%) increased, probably due to a volumetric change of the solvent, and no significant change of its shape was observed. If the conformation of **5c** is the zigzag type as observed in the solid state of **5a** and **5b**, the helical chirality generated between the anthracene moiety and the naphthalene moieties above and down cancels each other out (Figure 8). It is essential to have helical structures to generate induced CD. We tentatively postulate that introduction of a large chiral auxiliary at the imide nitrogen atom may change the pattern of folding from a symmetrical zigzag type to an asymmetric helical type.

After irradiation for 25 s with a high-pressure mercury lamp, the CD signal of **5c** disappeared almost completely (Figure 7b). The [4 + 4] photocycloaddition destroyed the overlapped π system of **5c** to afford **6c**, which results in annihilation of the induced CD as well as disappearance of yellow color. Thermal

(27) AM1 calculation was carried out by WinMOPAC Ver. 3 (Fujitsu, Ltd.). Stewart, J. J. P. *J. Comput. Chem.* **1989**, *10*, 209–220 and 221–264.

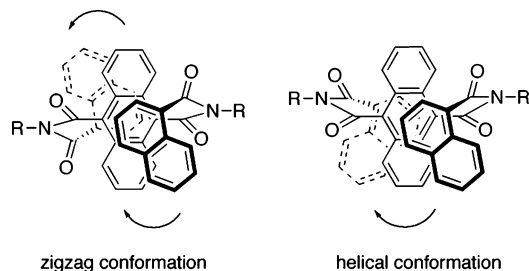


FIGURE 8. Two possible conformations, zigzag and helical conformations, of S-shaped foldamers.

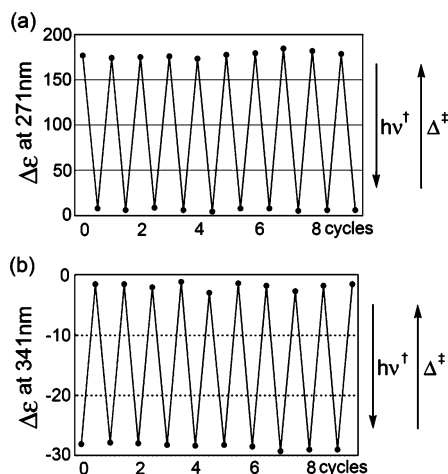


FIGURE 9. CD spectral changes ($\Delta\epsilon$) observed at 271 (a) and 341 nm (b) in chiral photochromic cycles between **5c** and **6c**. †The solution of **5c** (5.1×10^{-5} M) was irradiated (>290 nm) for 25 s and then ‡heated for 20 min at 60°C in an alternate way.

reversion (heating for 20 min at 60°C) of **6c** revealed complete recovery of the CD spectrum of the starting **5c**. The results indicated that the original helical conformation of **5c** was regenerated completely after heating. Figure 9a and 9b shows reversible photochromic cycles for **5c**–**6c** (irradiation and heating were carried out alternately) presented by the CD spectral changes ($\Delta\epsilon$) at 341 and 271 nm, respectively. Good reversibility was observed. Some sterically constrained molecules have been known to undergo ring opening. The norbornadiene–quadricyclane cycle²⁸ is a good example of a ring-strain-driven T-type photochromic system. The driving force for our cycloreversion is possibly similar to this, the steric constraint generated by cycloaddition. The [4 + 4] photocycloaddition of **5c** gives bi-planemer-²⁹type adduct **6c** which thrusts its planes up- and downward, causing steric compression on the remaining naphthoyl moiety. Due to this steric constraint, the retro cycloaddition of cycloadducts might occur to release the steric energy. The bulky substituents at the imide nitrogen atom might regulate conformational equilibrium between the two helical foldamers.

We demonstrated a novel T-type chiral photochromic system utilizing [4 + 4] photocycloaddition reaction of sterically constrained aromatic foldamers.

(28) (a) Dauben, W. G.; Cargill, R. L. *Tetrahedron* **1961**, *15*, 197–201. (b) Garman, A. A.; Leyland, R. L. *Tetrahedron Lett.* **1972**, *13*, 5345–5348. (c) Franceschi, F.; Guardigli, M.; Solari, E.; Floriani, C.; Chiesi-Villa, A.; Rizzoli, C. *Inorg. Chem.* **1997**, *36*, 4099–4107.

(29) Kimura, M.; Sirasu, K.; Okamoto, H.; Satake, K.; Morosawa, S. *Tetrahedron Lett.* **1992**, *33*, 6975–6978.

Experimental Section

Synthesis of Aromatic Imides 5. *N*-(Benzyl){10-[*N*-(benzyl)-*N*-(naphthylcarbonyl)carbomoyl](9-anthryl)}-*N*-(naphthylcarbonyl)carboxamide **5a**. Thionyl chloride (2.75 mL, 37.9 mmol) was added to 9,10-anthracenedicarboxylic acid (500 mg, 1.88 mmol) in dry toluene (35 mL). After the solution was refluxed with stirring for 17 h, excess thionyl chloride and toluene was evaporated. Benzylamine (0.431 mL, 3.95 mmol), DMAP (483 mg, 3.95 mmol), and dry toluene (40 mL) were added to the flask, and then the solution was refluxed with stirring for 6 h. After cooling to room temperature, the precipitate was filtered and the filtrate washed with ethyl acetate to give anthracene-9,10-dicarboxylic acid bis-benzylamide as a white powder. No further purification was necessary. Yield: 369 mg (44%); mp 247 – 249°C . This diamide (350 mg, 0.787 mmol) and DMAP (211 mg, 1.73 mmol) were dissolved into dry pyridine (20 mL) and toluene (30 mL) under reflux. To the resulting mixture, 1-naphthoyl chloride (0.300 mL, 1.99 mmol) was added. The resulting solution was refluxed for an additional 39 h with stirring. After cooling to room temperature, drops of concentrated HCl were added to the solution until the pH of the solution became 4–5. Then, the solution was washed with diluted HCl and brine. The organic layer was dried over MgSO_4 , filtered, and evaporated. The residues were recrystallized from chloroform–hexane to give **5a** as yellow crystals (202 mg, 34%): mp 220 – 222°C . UV–vis (CHCl_3) 268 (12 000), 326 (3200), 402 (2700), 421 (3000) nm. ^1H NMR (CDCl_3 , 400 MHz) δ 7.77 (d, $J = 7.3$, 4H), 7.48 (t, $J = 7.3$, 4H), 7.41 (t, $J = 7.3$, 2H), 7.24–7.14 (m, 10H), 7.09 (t, $J = 7.6$, 2H), 6.85 (d, $J = 8.2$, 2H), 6.63 (t, $J = 7.6$, 2H), 6.41 (d, $J = 8.2$, 2H), 6.32 (d, $J = 6.4$, 2H), 6.15 (t, $J = 7.6$, 2H), 5.48 (s, 4H). ^{13}C NMR (CDCl_3 , 100 MHz) δ 173.3, 170.6, 137.0, 132.0, 131.8, 131.7, 130.3, 129.2, 128.8, 128.2, 128.0, 126.7, 126.5, 126.4, 125.6, 125.1, 124.7, 122.9, 122.3, 47.9. MS (FAB) m/z 753 [MH^+]. Anal. Calcd for $\text{C}_{52}\text{H}_{36}\text{N}_2\text{O}_4 \cdot \text{H}_2\text{O}$: C, 81.02; H, 4.97; N, 3.63. Found: C, 80.73; H, 4.76; N, 3.65. Crystallographic data for **5a**: triclinic, $P-1$, $a = 9.0732(10)$ Å, $b = 10.0821(11)$ Å, $c = 10.6590(12)$ Å, $\alpha = 87.530(2)^\circ$, $\beta = 85.689(2)^\circ$, $\gamma = 70.442(2)^\circ$, $V = 916.03(18)$ Å³, $Z = 1$, $D_c = 1.365$ mg m^{-3} , $T = 150$ K, $\mu = 0.086$ mm⁻¹, GOF on $F^2 = 1.061$, $R_1 = 0.0454$, $wR_2 = 0.1105$ ($[I > 2\sigma(I)]$).

N-(2-Methylbenzyl){10-[*N*-(2-methylbenzyl)-*N*-(naphthylcarbonyl)carbomoyl](9-anthryl)}-*N*-(naphthylcarbonyl)carboxamide **5b**. In a similar way as for the synthesis of **5a**, **5b** was prepared in 37% yield as yellow crystals (chloroform–hexane): mp 265 – 267°C . UV–vis (CHCl_3) 270 (24 601), 322 (6962), 400 (5258), 421 (5641) nm. ^1H NMR (CDCl_3 , 500 MHz) δ 7.73 (d, $J = 6.7$, 2H), 7.32–7.24 (m, 17H), 7.3 (t, $J = 7.3$, 2H), 6.89 (d, $J = 8.2$, 2H), 6.48 (d, $J = 6.7$, 2H), 6.43 (d, $J = 8.55$, 2H), 6.20 (t, $J = 7.6$, 2H), 5.53 (s, 4H), 2.65 (s, 6H). ^{13}C NMR (CDCl_3 , 125 MHz) δ 173.2, 170.5, 136.9, 135.1, 132.0, 131.8, 131.7, 130.7, 130.0, 129.5, 128.0, 127.9, 126.6, 126.5, 126.4, 126.2, 125.5, 125.2, 124.8, 122.7, 122.3, 44.8, 19.8. MS (FAB) m/z 780 [M^+]. Anal. Calcd for $\text{C}_{53}\text{H}_{38}\text{N}_2\text{O}_4 \cdot 0.5\text{H}_2\text{O}$: C, 82.04; H, 5.07; N, 3.61. Found: C, 82.33; H, 5.09; N, 3.55. Crystallographic data for **5b**: triclinic, $P-1$, $a = 9.0414(7)$ Å, $b = 9.4957(7)$ Å, $c = 13.2099(10)$ Å, $\alpha = 103.9160(10)^\circ$, $\beta = 97.8330(10)^\circ$, $\gamma = 110.0190(10)^\circ$, $V = 1004.17$ (13) Å³, $Z = 1$, $D_c = 1.295$ mg m^{-3} , $T = 150$ K, $\mu = 0.081$ mm⁻¹, GOF on $F^2 = 1.050$, $R_1 = 0.0585$, $wR_2 = 0.01486$ ($[I > 2\sigma(I)]$).

N-((1*S*)-1-Phenylethyl){10-[*N*-((1*S*)-1-phenylethyl)-*N*-(naphthylcarbonyl)carbomoyl](9-anthryl)}-*N*-(naphthylcarbonyl)carboxamide **5c**. In a similar way as for the synthesis of **5a**, **5c** was prepared in 75% yield as yellow crystals (from chloroform–hexane): mp 255 – 257°C . UV–vis (CHCl_3) 273 (13 000), 329 (3700), 400 (2700), 421 (3000) nm. ^1H NMR (CDCl_3 , 500 MHz) δ 8.67 (br d, $J = 7.1$, 2H), 7.93 (br s, 2H), 7.89 (br d, $J = 7.9$, 2H), 7.81 (br t, $J = 6.7$, 2H), 7.75 (br d, $J = 6.4$, 2H), 7.59 (ddd, $J = 8.3$, 7.3, 0.8, 4H), 7.48 (br s, 2H), 7.44 (br s, 2H), 7.40 (br s, 2H), 7.26 (br s, 2H), 7.21 (br q, $J = 6.7$, 2H), 7.18 (br s, 2H), 7.00 (br t, $J = 6.4$, 2H), 6.78 (br s, 2H), 6.50 (br t, $J = 7.2$, 2H), 6.24

(br d, $J = 6.5$, 2H), 5.95 (br d, $J = 5.5$, 2H), 5.79 (br s, 2H), 2.43 (br d, $J = 4.9$, 6H). ^{13}C NMR (CDCl_3 , 125 MHz) δ 173.5, 168.8, 133.8, 132.0, 131.8, 131.6, 129.39, 129.36, 128.7, 128.3, 127.83, 127.79, 126.5, 126.5, 126.2, 126.0, 125.8, 125.6, 125.4, 125.2, 125.1, 124.8, 123.4, 122.5, 122.4, 121.8, 51.0, 18.2. HRMS (FAB) calcd for $\text{C}_{62}\text{H}_{44}\text{N}_2\text{O}_4$ [M^+] 880.3375, found 880.3301.

Structural Elucidation of [4 + 4] Photocycloadducts. Since the [4 + 4] photocycloadducts were thermally unstable due to the retro cycloreversion to the original imides, structural elucidation was carried out on the irradiated sample immediately after irradiation by ^1H NMR spectroscopy. Their spectra were compared with those of the similar reported system. In a typical run irradiation was carried out externally with a 400 W high-pressure mercury lamp for 10 min in an ice–water bath on the sample of carboxamide **5** (ca. 20 mg) in CDCl_3 (ca. 0.6 mL).

^1H NMR (CDCl_3 , 500 MHz) spectra of **6a**: δ 8.43 (d, $J = 8.6$, 1H), 7.99 (d, $J = 8.0$, 1H), 7.92 (d, $J = 8.3$, 1H), 7.68–7.24 (m, 17H), 7.05–6.88 (m, 4H), 6.74–6.65 (m, 4H), 6.37 (d, $J = 7.4$, 1H), 5.98 (t, $J = 7.7$, 1H), 5.75 (d, $J = 7.7$, 1H), 5.24 (d, $J = 7.4$, 1H), 5.17 (d, $J = 13.8$, 1H), 5.09 (d, $J = 13.8$, 1H), 4.04 (d, $J = 14.0$, 1H), 4.00 (d, $J = 14.0$, 1H).

^1H NMR (CDCl_3 , 500 MHz) spectra of **6b**: δ 8.31 (d, $J = 8.4$, 1H), 8.05 (d, $J = 8.2$, 1H), 7.98 (d, $J = 8.2$, 1H), 7.88 (d, $J = 6.8$, 1H), 7.68 (m, 2H), 7.61 (t, $J = 7.2$, 1H), 7.44 (m, 1H), 7.34 (d, $J = 7.0$, 1H), 7.28 (m, 4H), 7.18–7.00 (m, 5H), 6.92 (t, $J = 7.2$, 1H), 6.83 (t, $J = 7.5$, 2H), 6.77–6.67 (m, 6H), 6.46 (m, 1H), 6.01 (t, $J = 7.9$, 1H), 5.78 (d, $J = 8.2$, 1H), 5.18 (d, $J = 14.5$, 1H), 5.11 (d, $J = 14.5$, 1H), 4.13 (d, $J = 16.6$, 1H), 4.07 (d, $J = 16.6$, 1H), 2.61 (s, 3H), 1.40 (s, 3H).

Since the ^1H NMR spectrum after irradiation of **5c** was complicated due to formation of the [4 + 4] cycloadduct **6c** (major) together with the minor diastereomeric cycloadduct and **5c** generated by retro cycloreversion, assignment of the peaks of the major isomer **6c** was carried out based on the COSY spectrum of the irradiated mixture. The diastereomeric ratio of cycloadducts was 95:5 based on integration of the methyl groups. ^1H NMR (CDCl_3 , 500 MHz) spectra of **6c** (major diastereomer): δ 8.47 (d, $J = 8.6$, 1H), 8.38 (d, $J = 8.3$, 1H), 8.09 (d, $J = 7.3$, 1H), 8.00 (t, $J = 8.4$, 2H), 7.95 (d, $J = 8.2$, 1H), 7.90 (d, $J = 8.2$, 1H), 7.8–7.1 (m, 18H), 6.63 (q, $J = 7.0$, 1H), 6.49 (br m, 2H), 6.35 (br m, 1H), 6.26 (br d, $J = 8.2$, 1H), 5.97 (d, $J = 7.4$, 1H), 5.86 (t, $J = 7.3$, 1H), 5.69 (d, $J = 7.7$, 1H), 5.56 (t, $J = 7.8$, 1H), 5.54 (d, $J = 8.3$, 1H), 5.41 (t, $J = 7.4$, 1H), 5.22 (q, $J = 6.7$, 1H), 4.97 (d, $J = 7.3$, 1H), 2.22 (d, $J = 7.1$, 3H), 1.45 (d, $J = 6.7$, 3H).

Absorption and CD Spectral Measurements after Irradiation. The solution of **5c** (5.1×10^{-5} M) in a cuvette with a stopcock was irradiated externally with a 100 W high-pressure mercury lamp with a Pyrex filter (<290 nm) at ambient temperature (ca. 25 °C) in CHCl_3 . Absorption and CD spectra of the irradiated sample were measured at certain intervals.

Supporting Information Available: Copies of ^1H NMR spectroscopic data of **5a–c** and **6a–c** (PDF) and crystallographic information files (CIF) and ORTEP diagrams (PDF) of **5a** and **5b**. This material is available free of charge via the Internet at <http://pubs.acs.org>.

JO0611317